CHLORIDE TRANSPORT IN TOAD SKIN (*BUFO VIRIDIS*)

THE EFFECT OF SALT ADAPTATION

By URI KATZ

Department of Biology, Technion, Haifa, Israel

and E. HVIID LARSEN

Zoophysiological Laboratorium A, University of Copenhagen, DK-2100 Copenhagen, Denmark

SUMMARY

1. The steady-state Cl^- current across the skin of *Bufo viridis* adapted to tap water was found to be rectified. In skins bathed with NaCl Ringer on both sides, a large outward current, carried by influx of Cl^-, was observed at a clamping voltage (V) of $< -50\,mV$ (outside of the skin negative). For $V = -50\,mV$ the transepithelial Cl^- conductance calculated from isotope flux measurements was $2 \cdot 5 \pm 0 \cdot 3\,mS\,cm^{-2}$, $N = 10$. When the skin was clamped at $+50\,mV$ the net flux of Cl^- was reversed, but Cl^- conductance was only $0 \cdot 3 \pm 0 \cdot 1\,mS\,cm^{-2}$. Flux ratio analysis indicated that the potential-activated Cl^- conductance carries Cl^- ions by way of passive transport.

2. With NaCl Ringer bathing the outer surface of the skin the spontaneous potential was about $-30\,mV$. At this potential the Cl^- conductance of the skin was about half of its maximum value.

3. The time course of Cl^- current activation following a fast, stepwise change of V from $50\,mV$ to a potential below $0\,mV$ showed an initial delay of a few seconds, and proceeded with a halftime ($T_{1/2}$) which varied as a bell-shaped function of V. The maximum $T_{1/2}$ was about $100\,s$ for $V = -10\,mV$ in skins exposed to KCl Ringer on the outside.

4. Following adaptation of the toads to a $250\,mM$-NaCl solution, the fully activated Cl^- conductance of the skin was greatly reduced, and the conductance-voltage curve was shifted to the left along the voltage-axis. With NaCl Ringer on the outside the spontaneous potential was about $-20\,mV$, and Cl^- conductance activation was possible only outside the physiological range of potentials. The time constant of Cl^- conductance activation from closed to fully activated state was more than doubled following salt adaptation of the toads.

5. The active inward Cl^- flux disappeared in skins of toads adapted to a $250\,mM$-NaCl solution, and apparent leakage conductance was reduced.

6. Application of the phosphodiesterase inhibitor 3-isobutyl-1-methylxanthine to skin of fully salt-adapted toads increased the transepithelial Cl^- conductance, and the time courses of voltage clamp currents became more like those of water-adapted toads. Apparent leakage conductance was increased.

7. Salt adaptation of *B. viridis* was followed by a statistically significant reduction in the number of mitochondria-rich cells relative to the number of granulosum cells of the replacement layer, from a ratio of 0·50 to 0·25. The volume of the mitochondria-rich cells was reduced following salt adaptation of the toads.

INTRODUCTION

The green toad, *Bufo viridis*, is one of the few euryhaline amphibians. Adaptation to high salinities is associated with an increase in the osmolarity of the body fluids, the plasma being hyperosmotic to the external bath. At all salinities to which the animal can adapt, Na^+ and Cl^- are the major osmotic constituents of the extracellular fluid, but at high salinities urea also contributes significantly to the total osmotic pressure (Katz, 1973*a*). Furthermore, transport properties of the skin are changed (Katz, 1979). The active sodium transport is greatly reduced (Katz, 1975), and an active uptake of urea is induced (Katz, Garcia-Romeu, Masoni & Isaia, 1981). Chloride conductance appears to be decreased (Katz, 1975).

Studies of Cl^- transport in the skin of *B. bufo* (Larsen & Kristensen, 1978; Larsen, 1982) and of *Rana esculenta* (Kristensen, 1983) provided evidence that the trans-epithelial Cl^- permeability depends on the potential across the skin, probably because Cl^--channels in an outward-facing membrane are gated by membrane potential (Larsen & Rasmussen, 1982). An implication of these studies is that Cl^- transport by toad skin cannot be studied by the conventional short-circuiting technique because the Cl^- conductance is almost completely deactivated at $V = 0\,mV$. As the Cl^- conductance becomes activated in the physiological region of transepithelial potentials and is fully activated in the hyperpolarizing region of the current-voltage relationship, investigation of the Cl^- transporting capacity of the skin requires voltage clamp analysis spanning a wider range of potentials. Such a technique was used in the present study to characterize the Cl^- transport systems in the skin of water-adapted *B. viridis* and to investigate their response to salt adaptation of the animal.

METHODS

Animals

Toads (*Bufo viridis*) of both sexes were collected in Israel near Jerusalem and were shipped to Copenhagen. Toads obtained from Saltholm island in Øresund, Denmark were used occasionally. Adaptation to NaCl solutions was carried out gradually. After 4–5 days in 115 mM-NaCl, the toads were transferred to 200 or 250 mM-NaCl solution. Some toads were transferred from tap water to 135 mM-NaCl and kept there for more than 10 days before analysis of transport through the isolated skin took place. The toads were fed prior to, but not during, adaptation. As judged by the size of fat bodies, all of the toads were in good feeding condition. Abdominal skins were used for analysis, and care was taken to use skins only in their intermoult period. All experiments were carried out at room temperature.

Measurements of ^{36}Cl fluxes in voltage clamped membranes

The skin was mounted in Perspex chambers with an exposed area of 7 cm^2. The rim

f the chamber was designed to minimize edge damage without employing chemicals for sealing (Koefoed-Johnsen, Ussing & Zerahn, 1952). The paracellular fluxes of Na^+ and Cl^- correspond to permeabilities of the order of 10^{-8} cm s^{-1} with an associated conductance of less than 100 μS cm^{-2} (Bruus, Kristensen & Larsen, 1976). K^{36}Cl or Na^{36}Cl was added to one of the bathing solutions to an activity of 4–20 μCi/20 ml depending on the expected magnitude of fluxes. After an initial equilibration period of 30–45 min, samples of 3 ml were taken at 20-min intervals from the opposite chamber. At each clamping potential samples were taken to provide four flux periods, the first being omitted for calculation of fluxes. Each sample was replaced with 3 ml activity-free Ringer and transferred to counting vials containing 10 ml scintillator cocktail (5 g PPO, 500 ml Triton X-100 *ad* 1000 ml toluol). For measurements of the (time independent) specific activity of Cl$^-$ in the 'hot' chamber two or three samples of 50 μl each were taken at appropriate intervals, and each sample was added to 3 ml Ringer and transferred to a vial for counting. When influx and efflux were measured simultaneously, paired membranes from either side of the ventral midline were employed.

The transepithelial potential was measured using calomel electrodes connected to the chamber *via* polyethylene tubes containing 300 mM-KCl-3 % agar, and located 2 mm from the inner and outer surfaces of the skin. Electrode asymmetries less than 200 μV were accepted without being nullified. Currents were passed through the skin *via* Ag/AgCl half-cells located either in the chambers or connected to the chambers *via* polyethylene bridges of the type used for potential measurements. The transepithelial potential was clamped automatically by a feedback circuit with a rise time of the command voltage of 100 ms. Automatic correction was made for solution resistance. Current and potential were recorded by a chart recorder. For high precision monitoring of the total charge flow through the membrane during each of the flux periods, the current was time-integrated and read out on a digital meter.

Monitoring the time course of voltage clamp currents and measurement of the conductance

The skin was mounted horizontally in a chamber of 2 cm^2 exposed area which allowed for a continuous perfusion of the outer surface of the preparation. The rim of this chamber was designed as that of the flux chamber, but due to the larger circumference-to-area ratio the leakage conductance is expected to be somewhat larger. The outer current electrode was replaced by a platinum wire, and all experiments were performed with a continuous flow of Ringer through the outer chamber. A fast feedback circuit providing a rise time of 10 μs for potential displacements was used. Current and potential were continuously monitored by a pen recorder and, when a better time resolution was needed, also on a storage oscilloscope or transient recorder. Slope conductance was measured by applying a 500 ms pulse (ΔV) of 20 mV amplitude to produce a current response (ΔI). G_{slope} was calculated as $\Delta I / \Delta V$. In skins exposed to K$^+$-Ringer outside, the current responses to brief potential pulses (500 ms) are linearly related to ΔV in the positive as well as in the negative region of the current-voltage curve.

Counting of mitochondria-rich cells

For histological quantification of the mitochondria-rich (m.r.) cells of the skin,

pieces were fixed according to Champy & Maillet (Gabe, 1968) which clearly distin
guishes the m.r. cells from the other cells. Osmolarities of fixation solutions were
adjusted with mannitol to be similar to that of toad plasma (250 and 500 mosmol l^{-1}).
Sections (10 μm) were examined in the light microscope. Four random fields of
200 μm length were selected from each piece of skin and visualized at $\times$1000. The two
cell types (m.r. and granulosum cells) of the cell layer beneath the stratum corneum
were counted, and their size measured with an eyepiece which had 100 divisions along
0·1 mm.

Solutions

The toad (high bicarbonate) Ringer contained (in mM): $Na^+ = 115$; $K^+ = 3$;
$Ca^{2+} = 2$; $Mg^{2+} = 0.5$; $Cl^- = 100$; $HCO_3^- = 20$; acetate $= 3$; gassed with 5%
$CO_2/95\% O_2$; pH $= 7.8$. The bicarbonate concentration is similar to that in frog
plasma (25 mM: Conway, 1957). The inner surface of the skin was exposed to toad
Ringer or, in some experiments with skins from toads adapted to 250 mM-NaCl, to a
Ringer (modified by adding 65 mmol l^{-1} NaCl and 150 mmol l^{-1} urea) which is similar
in composition and osmolarity to the plasma of toads fully adapted to 250 mM-NaCl
(Katz, 1973a,b). The outer surface was exposed either to toad Ringer or to Ringer
solutions in which gluconate or sulphate replaced chloride, and potassium replaced
sodium, the osmolarity being kept constant. The skin was equilibrated for at least 1 h
with the serosal solution before the experimental analysis started.

A 'low bicarbonate' Ringer, as normally used in studies of isolated amphibian skin,
was used for some experiments, where stated (Figs 1, 2, 3 and Table 1), in order to
compare results with previously published experiments with *Bufo bufo*. The com-
position of this Ringer was (in mM): $Na^+ = 115$; $K^+ = 2.4$; $Ca^{2+} = 1$; $Cl^- = 114$;
$HCO_3^- = 2.4$; acetate $= 3$; gassed with atmospheric air; pH $= 8.2$.

The phosphodiesterase inhibitor 3-isobutyl-1-methyl-xanthine (IBMX) was ob-
tained from Sigma.

Voltage and current reference

The transepithelial potential, V, is given as the potential in the outer bath minus
that in the inner bath. Inward going currents are defined positive.

RESULTS

The conductive chloride pathway in the skin of water-adapted Bufo viridis

The potential dependence of the steady-state current (I^∞) in a skin exposed to NaCl
Ringer on its inner and outer surfaces is shown in Fig. 1A. The I^∞-V curve is non-
linear with large currents for V < 0 mV. Replacement of the Cl^- ions in the outer bath
by gluconate eliminated the greater part of the outward currents (Fig. 1A), suggesting
a high Cl^- ion specificity of the outward going rectifier. Replacement of Na^+ by K^+
in the outer chamber did not alter significantly the outward currents, but they were
reduced by one order of magnitude when Cl^- was also removed (Fig. 1B). Following
this ion substitution, the current-voltage curve of the preparation was linear. These
results indicate that the Cl^- conductance varies with the transepithelial potential in

such a way that it passes large outward currents carried by an inward flux of Cl^- for
$V < 0$ mV. To verify this, the potential dependence of the Cl^- current was analysed by
measurements of unidirectional Cl^- fluxes as a function of transepithelial potential.
Provided the influx (J_{Cl}^{in}) and efflux (J_{Cl}^{out}) are measured at the same clamping potential,
the Cl^- current (I_{Cl}) is given by, $I_{Cl} = -F (J_{Cl}^{in} - J_{Cl}^{out})$, where F is the Faraday. A
representative range of results are illustrated in Fig. 2. In Fig. 2A, left-hand panel, the
inwardly-directed Cl^- current (carried by an outwardly-directed net flux of Cl^- ions)
is small in spite of the large driving force of 50 mV. It can be seen that the clamping
current at this potential is carried by some ions other than Cl^- (probably Na^+). As
expected, clamping to -50 mV is associated with reversal of the Cl^- current. At this
potential, however, the Cl^- current accounts for almost all of the clamping current,
and its absolute magnitude is significantly larger than at 50 mV. Assuming that the
driving force of transepithelial Cl^- ion flow is derived from no other source than the
electrochemical potential difference between Cl^- in the inner and outer bathing
solutions (see below), and with equal Cl^- activities in these solutions, the passive Cl^-
conductance (the steady state chord conductance) is given by, $G_{Cl} = I_{Cl}/V$. In the
example of Fig. 2A, G_{Cl} is increased from 0.06 mS cm^{-2} to 2.5 mS cm^{-2}, i.e. 40-fold,
following a change in V from $+50$ to -50 mV. Returning V to 50 mV, the steady state
Cl^- fluxes relax close to their initial values ($G_{Cl} = 0.08$ mS cm^{-2}), illustrating the
reversibility of the Cl^- conductance activation. In the preparation of Fig. 2B, V was
clamped at -100 mV in the final period, instead of being stepped back to 50 mV, giving
conductance values (mS cm^{-2}) of 0.05 (50 mV), 0.88 (-50 mV), and 2.16
(-100 mV). This reveals a strong V-dependence of the transepithelial Cl^- conduc-
tance, although the Cl^- conductance at -50 mV was considerably smaller than that of
the example given above. In the experiment of Fig. 2C, there was a significant Cl^-
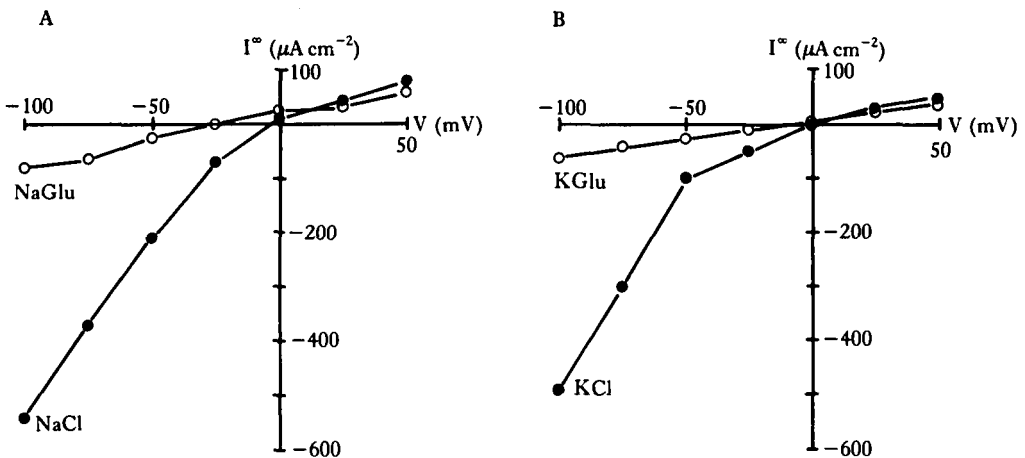conductance at 50 mV ($G_{Cl} = 0.5$ mS cm^{-2}), and the Cl^- conductance was increased

Fig. 1. Steady-state current-voltage (I^∞-V) curves of the isolated skin of water-adapted *Bufo viridis*
bathed with NaCl Ringer (2.4 mM-bicarbonate) on its inner surface. (A) Na^+ Ringer on the outside
either with Cl^- (●) or gluconate (○) as the major anion. (B) K^+ Ringer on the outside either with Cl^-
(●) or gluconate (○) as the major anion. Notice that the large outward currents for $V < -50$ mV
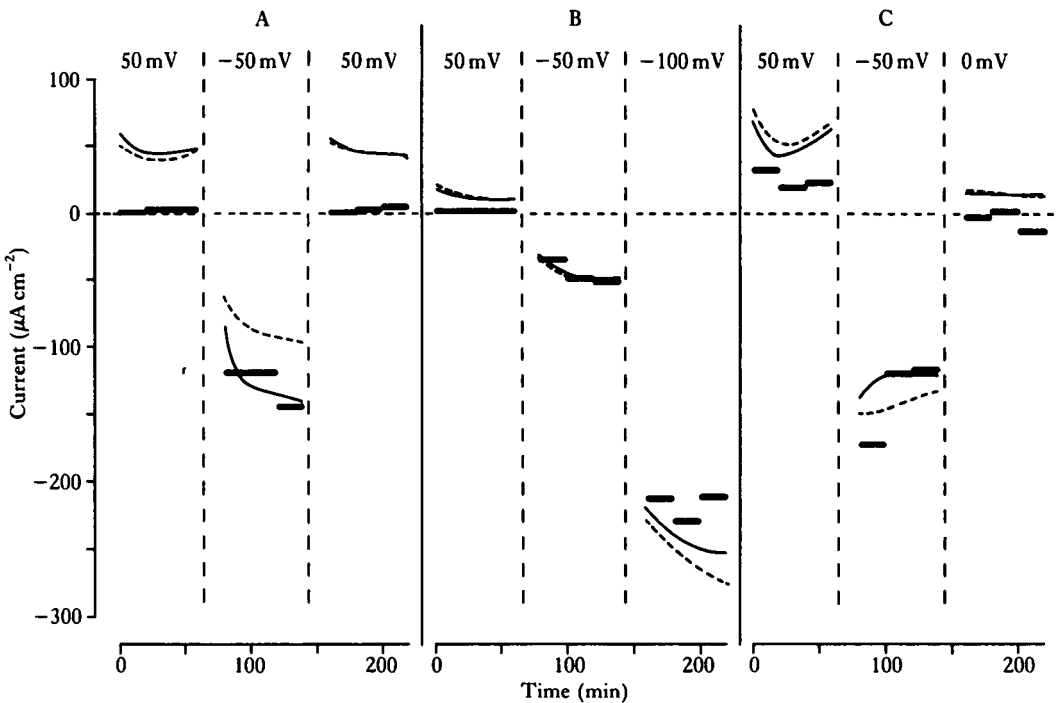depend on the presence of Cl^-, but not Na^+, in the outside solution.

Fig. 2. Potential dependence of transepithelial total currents (curves) and Cl⁻ currents (horizontal bars, calculated from measurements of ³⁶Cl fluxes). NaCl Ringer with 2·4 mM-bicarbonate on both sides of the preparations. Results shown in panels A, B and C are from experiments with skins of three different toads. Influx and efflux of Cl⁻ were measured on symmetrical belly skins from the same animal. The currents of both preparations are given (————, influx skin; – – –, efflux skin). At times indicated by a vertical dashed line the potential was changed to the value indicated. The first 20 min flux value at each clamping potential is omitted as are the initial current responses to the shift in potential, the later being exemplified in Fig. 3.

by bringing the potential to -50 mV ($G_{Cl} = 2\cdot7$ mS cm^{-2}). At V = 0 mV, the net flux of Cl⁻ was close to zero.

From the results it can be concluded that the Cl⁻ conductance in the skin of *B. viridis* exhibits a strong V-dependence, being significantly activated in the negative region of the current-voltage relationship, and deactivated following reversal of V with respect to its physiological polarity (Table 1). The flux-ratios indicate that the activated conductance carries Cl⁻ ions predominantly by passive transport, whereas chloride transport at V = 50 mV is also governed by active transport or exchange diffusion, or both. However, as the flux-ratio at V = 0 mV reveals passive transport only (Table 1), contribution from an active pathway is probably very small. Thus, the results of the flux-ratio analysis justify the use of the equation above for calculation of G_{Cl}. In these experiments with low bicarbonate Ringer the small short-circuit current (Table 1) is within the range of values obtained in the skin of *B. bufo* also exposed to a low bicarbonate Ringer on both sides (Bruus *et al.* 1976).

The instantaneous current response to a hyperpolarizing potential pulse was followed by a time-dependent stimulation of an outward current component

Table 1. *Potential dependence of unidirectional Cl⁻ fluxes, Cl⁻ current (I$_{Cl}$), clamping current (I$_t$, taken from influx skins), Cl⁻ conductance (G$_{Cl}$), and ratio of Cl⁻-fluxes of skins of water-adapted toads*

Clamping potential (N)	−50 mV (10)	0 mV (7)	+50 mV (12)
J_{Cl}^{in} (nmol cm^{-2} min^{-1})	91·2 ± 12·8	17·6 ± 3·7	5·19 ± 1·36
J_{Cl}^{out} (nmol cm^{-2} min^{-1})	11·9 ± 2·5	16·0 ± 3·0	14·9 ± 3·1
I_{Cl} (μA cm^{-2})	−127 ± 17	−3·5 ± 2·7	14·7 ± 6·2
I_t (μA cm^{-2})	−119 ± 17	9·8 ± 2·3	49·2 ± 6·4
G_{Cl} (mS cm^{-2})	2·5 ± 0·3	–	0·3 ± 0·1
J_{Cl}^{in}/J_{Cl}^{out} (observed)	9·4 ± 1·6	1·08 ± 0·14	0·71 ± 0·26
J_{Cl}^{in}/J_{Cl}^{out} (theoretical)	7·1	1	0·14

The skins were exposed to NaCl Ringer (2·4 mM-HCO$_3^-$) on the inside and outside.

The theoretical flux-ratios were calculated from (Ussing, 1949): $J_{Cl}^{in}/J_{Cl}^{out} = \exp(-FV/RT)$, where $F/RT = 39.4 \times 10^{-3}$ mV^{-1}.

The spontaneous potentials of skins clamped at V = 0 mV were (N = 7), −7·8 ± 3·1 mV (influx skins) and −9·1 ± 2·8 mV (efflux skins), respectively.
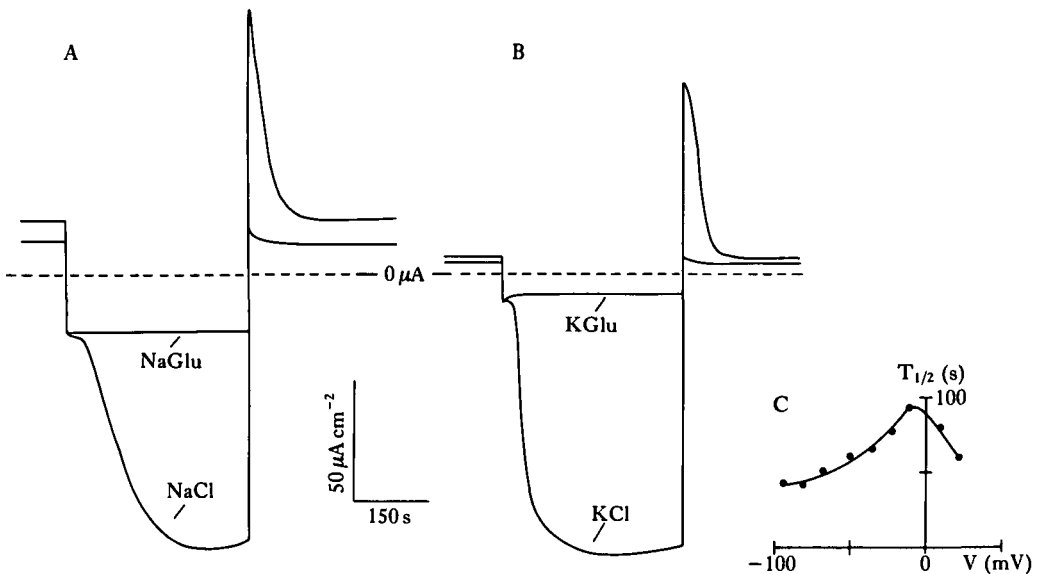
Mean ± S.E. with N denoting number of preparations.

Fig. 3. Time course of voltage clamp currents of the skin of water-adapted *Bufo viridis*. NaCl Ringer (2·4 mM-bicarbonate) on the inside. The transepithelial potential was stepped from 50 to −60 mV and after 360 s at −60 mV, V was stepped back to the holding value of 50 mV. All of the records were obtained from the same skin preparation. The indicated current and time scale apply to the records of A as well as of B. (A) NaCl- or Na-gluconate Ringer on the outside. (B) KCl- or K-gluconate Ringer on the outside. Notice that the current activation at V = −60 mV requires the presence of Cl⁻ ions in the external bath. The time course of Cl⁻ current activation is slow, but fully reversible and is observed irrespective of the accompanying cation in the outer bath. (C) The time constant of current activation at a given clamping potential may be expressed by the time (T$_{1/2}$) it takes for the current to reach half of its maximum change following a shift of V from a holding potential where the membrane is deactivated. The graph shows the dependence of T$_{1/2}$ on the potential at which activation takes place. Holding potential, 50 mV. KCl Ringer on the outside, NaCl Ringer on the inside. It is seen that the rate of current activation increases with decreasing clamping potential for −100 < V < −10 mV. Provided the skin is isolated in the intermoult period the records of this figure are typically obtained in the skin of *Bufo viridis*. Similar current-time courses are obtained with skins of *Bufo bufo* (see text for references).

approaching a new steady state in the course of 200 s (Fig. 3). This current componeท was carried by an inward flux of Cl⁻ ions since no such current response was seen aftด the Cl⁻ ions of the outer bath were replaced by gluconate, but replacement of Na⁺ by K⁺ had no effect (compare Fig. 3A and B). Following a shift of V back to 50 mV the current slowly relaxed to its pre-pulse steady state value, confirming that potential activation of the Cl⁻ conductance is a fully reversible process.

$T_{1/2}$ values of the current-time curves are shown in Fig. 3C. The $T_{1/2}$-V curve is bell shaped with a maximum $T_{1/2}$ of about 100 s at a clamping potential of -10 mV, which is in good agreement with the hypothesis that the dynamic Cl⁻ current responses to voltage clamping are caused by a potential gated Cl⁻ permeability.

The time course and kinetics of voltage clamp currents of the skin of *B. viridis* are similar to those for *B. bufo* (Larsen & Rasmussen, 1982), showing that the conductive Cl⁻ pathways in these tissues are of a similar nature. This was found in both low and high bicarbonate Ringer. In the following experiments the 20 mM-HCO₃⁻ Ringer is used, and the study of changes of the Cl⁻ transport following salt adaptation is performed with this Ringer bathing the control as well as the 'salt-adapted' skins.
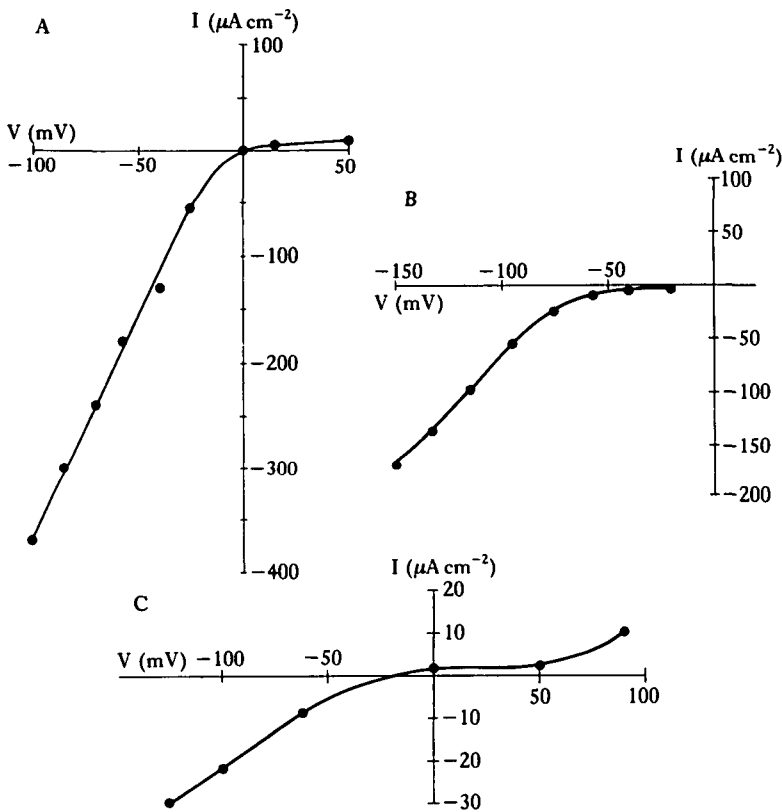

Fig. 4. Steady-state current-voltage curves of the isolated skin of *Bufo viridis*. NaCl Ringer on the inside, KCl Ringer (20 mM-HCO₃⁻ solutions) on the outside. (A) Skin of a water-adapted animal. (B) Skin of an animal kept in a 250 mM-NaCl solution for 6 days. (C) Skin of an animal kept in a 250 mM-NaCl solution for 12 days.

Effect of salt adaptation on the Cl⁻ conductive pathway

In the study of salt adaptation the preparation was bathed with KCl Ringer on the outside so that the outward currents ($V < 0$ mV) may be expected to be carried by an inward movement of Cl^- ions with only small contributions from other ionic components. Outward currents became significantly smaller following adaptation of the toads to a 250 mM-NaCl solution (Fig. 4), indicating that the gated Cl^- conductance gradually disappeared. This conclusion was substantiated by finding that Cl^- influx at -80 mV was 175 ± 38 nmol cm^{-2} min^{-1} (mean $\pm$ s.e., $N = 4$) in water-adapted toads, and 1.0 ± 0.16 nmol cm^{-2} min^{-1} in 250 mM-NaCl-adapted toads. This latter value corresponds to a current of $-1.6 \pm 0.3 \mu A$ cm^{-2}, which is significantly less than the clamping current at -80 mV indicated in Fig. 4C (at $V = -80$ mV, a mean value of $-22.4 \pm 5.6 \mu A$ cm^{-2} was obtained in seven skins of fully salt-adapted toads). This shows that the major current component is carried by some ions other than Cl^- at this potential. With an ohmic leakage conductance of 0.23 ± 0.09 mS cm^{-2} of skins of fully salt-adapted toads (Table 2), the leakage current at -80 mV is about $-18 \mu A$ cm^{-2}. This is close to the observed value. The ionic basis of the leakage currents was not
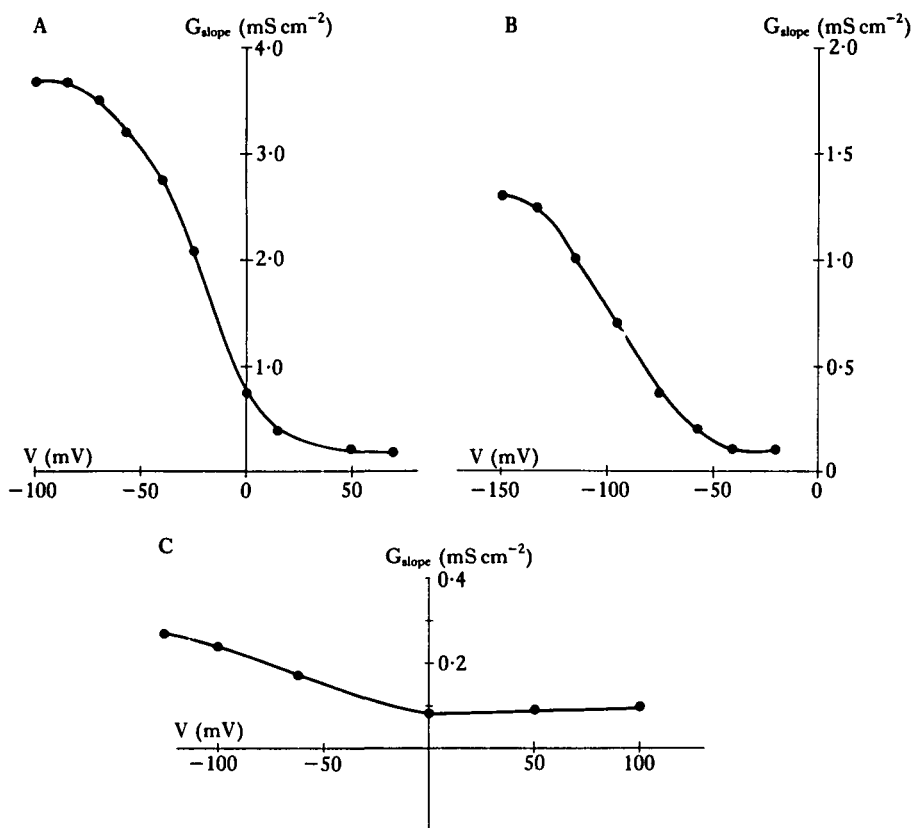

Fig. 5. Potential dependence on the slope conductance of the three preparations, the I$^\infty$-V curves of which are shown in Fig. 4. The slope conductances were calculated from the current responses to a 500 ms voltage pulse of 20 mV superimposed on the clamping potential at the time the steady-state currents were achieved. For pretreatments of the toads, see legend of Fig. 4.
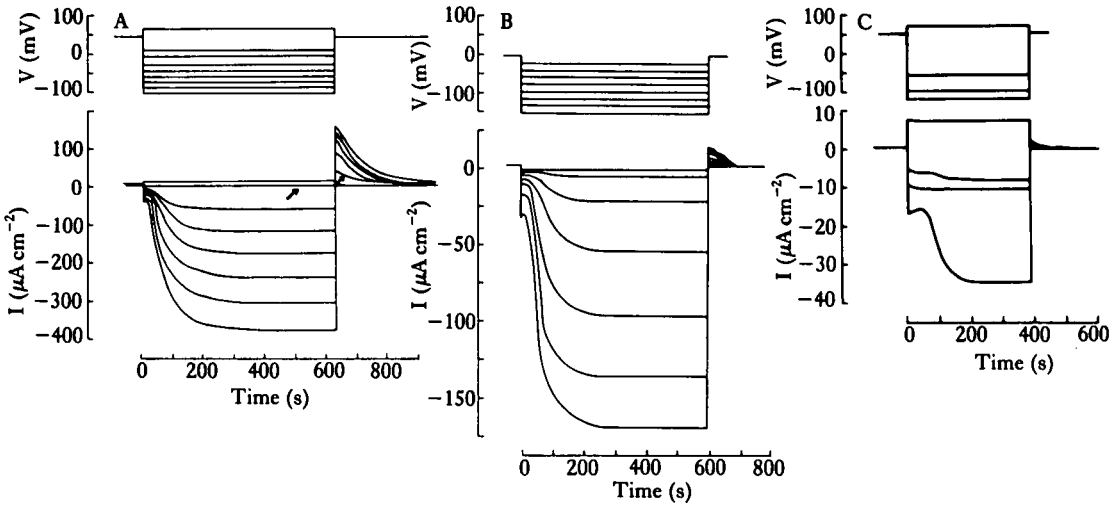
Fig. 6. Families of current-time curves in response to the voltage clamp protocols given on top. Same three preparations as in Fig. 4. (A) Skin of a water-adapted toad. Holding potential 50 mV. Note the significant 'off response' of the current (arrow) following return of V to the holding potential from 0 mV, despite the fact that no current is flowing while the preparation is clamped to 0 mV. This shows that the conductance change depends on potential and not on current flow. (B) Skin of a toad kept for 6 days in a 250 mM salt solution. Holding potential 0 mV. (C) Skin of a toad kept for 12 days in a 250 mM salt solution. Holding potential 50 mV.

identified in the present study. It is likely, however, that the leakage currents are carried by the major cations (Na^+ or K^+, depending on direction of current flow).

With KCl Ringer outside, the dynamic skin conductance was governed predominantly by the Cl^- permeability. Thus, the potential dependence of the gated Cl^- conductance can be estimated by measurements of the total conductance of the skin as a function of potential (see Methods). The conductance-voltage relationship of the skin of *B. bufo* is an inverted S-shaped graph with its steepest part between 0 mV and -50 mV (Larsen & Kristensen, 1978; Larsen & Rasmussen, 1982). A similar G_{slope}-V relationship was obtained with the skin of water-adapted *B. viridis* (Fig. 5A). Following adaptation to 250 mM-NaCl, the conductance-voltage curve was shifted to the left along the V-axis (Fig. 5B, C).

The Cl^- current activation showed an initial delay, irrespective of the pretreatment of the toads. This delay was significantly increased in skins of toads fully adapted to 250 mM-NaCl (see Fig. 6).

In the above experiments, the preparations from salt-adapted toads were bathed on the inside with Ringer having an osmolarity of 250 mosmol l^{-1}. Similar results were obtained when the inner solution was a 500 mosmol l^{-1} Ringer, having a composition similar to that of plasma of toads fully adapted to 250 mM-NaCl (compare Fig. 6C with Fig. 7A).

The effects of salt adaptation upon the voltage clamp currents are summarized in Table 2. Salt adaptation also reduced the spontaneous skin potential (V_{sp}), decreased short-circuit current (I_{sc}), and increased transepithelial short-circuit resistance (R_s

Table 2. *Summary of results comparing the electrical properties of skins of water-adapted toads (control) with those of toads fully adapted to a 135 and 250 mM-NaCl solution*

Condition of adaptation	H₂O	135 mM-NaCl	250 mM-NaCl
NaCl Ringer outside			
V_{sp} (mV)	−32·7 ± 7·4 (8)	−19·0 ± 4·5 (4)	−18·1 ± 3·2 (7)
I_{sc} (µA cm⁻²)	55·5 ± 4·9 (8)	10·1 ± 0·6 (4)	4·8 ± 2·1 (7)
R_{sc} (Ωcm²)	573 ± 94 (8)	2191 ± 309 (4)	5573 ± 1182 (7)
KCl Ringer outside			
G_{max} (mS cm⁻²)	2·22 ± 0·28 (10)	1·65 ± 0·60 (4)	0·61 ± 0·25 (7)
$T_{1/2}$ (s)	50·4 ± 8·4 (9)	73·2 ± 18 (4)	131 ± 27 (6)
$V_{1/2}$ (mV)	−31 ± 7 (5)	−67 ± 5 (4)	−88 ± 9 (4)
K-gluconate Ringer outside			
G_{leak} (mS cm⁻²)	0·44 ± 0·09 (10)	0·32 ± 0·22 (4)	0·23 ± 0·09 (4)

In all three experimental groups the isolated skins were exposed to NaCl Ringer solution (20 mM-HCO₃⁻) on the inside. The composition of the outside solution is indicated in the table.

V_{sp} = spontaneous skin potential.

I_{sc} = short-circuit current.

R_{sc} = skin resistance at 0 mV calculated from the current response to a V-pulse of 20 or 30 mV amplitude and 500 ms duration.

G_{max} = maximum slope conductance of the skin (cf. Fig. 5).

$T_{1/2}$ = half-time of current change from deactivated to fully activated Cl⁻ conductance.

$V_{1/2}$ = the potential at which the transepithelial slope conductance is half of its maximum value.

G_{leak} = slope conductance at V = 50 mV measured with K-gluconate Ringer outside.

Mean ± s.e. with the number of preparations in parenthesis.

(Table 2). The effects on I_{sc} and R_{sc} reflect the reduced Na⁺ permeability of the apical membrane as previously discussed (Katz, 1975). The short-circuit current in control skins (Table 2) was significantly higher than in skins exposed to low bicarbonate Ringer (Table 1).

The effect of salt adaptation on other pathways

In the short-circuited skin of tapwater-adapted *B. viridis* the Cl⁻ influx was significantly larger than the Cl⁻ efflux, showing inward going active transport of this ion (see Table 3). The mean value of the Cl⁻ net fluxes corresponds to a statistically significant ($P < 0.005$) current of $-20.4 \pm 8.2\,\mu\text{A cm}^{-2}$. A similar high rate of active Cl⁻ transport is seen in skin of the frog, *Leptodactylus ocellatus* (Zadunaisky, Candia & Chiarandini, 1963; Rotunno, Ques-von Petery & Cereijido, 1978). Adaptation of *B. viridis* to 250 mM-NaCl was followed by disappearance of the active pathway since the net flux of Cl⁻ for V = 0 mV was not significantly different from zero (Table 3).

Substitution of the Cl⁻ ions in the outer solution by SO₄²⁻ ions significantly reduced the Cl⁻ efflux (Table 3). A similar 'trans-effect' in short-circuited skins of *B. bufo* (Bruus *et al.* 1976; Kristensen & Larsen, 1978) and *Rana pipiens* (Biber, Walker & Mullen, 1980) was interpreted as due to exchange diffusion of Cl⁻. This hypothesis is consistent with a flux ratio analysis for *B. bufo* covering a large range of transepithelial potentials revealing large unidirectional Cl⁻ fluxes and almost zero Cl⁻ conductance for 0 mV < V < 50 mV (Larsen, 1982). For the frog skin, evidence has

Table 3. Cl^- fluxes of skins of water- and 250 mM-NaCl-adapted toads, respectively

| | Cl^- influx | Cl^- efflux (nmol cm^{-2} min^{-1}) | |
External anion	Cl^-	Cl^-	SO_4^{2-}
H_2O	21·7 ± 5·0	9·0 ± 2·2	1·8 ± 1·0
250 mM-NaCl	1·0 ± 0·16	1·0 ± 0·33	1·0 ± 0·50

NaCl Ringer's solution (20 mM-HCO$_3^-$) on the inside, and on the outside (first two columns), or Na$_2$SO$_4$-Ringer's solution (20 mM HCO$_3^-$) on the outside (last column).
All of the preparations were clamped at V = 0 mV.
Mean ± s.e. for N = 4 preparations of each group.

been presented that three-quarters of the efflux of Cl^- is not associated with a trans-epithelial conductance (Biber *et al.* 1980). However, in the skin of *R. temporaria* and *R. esculenta* (Kristensen, 1978, 1982), and *L. ocellatus* (Ques-von Petery, Rotunno & Cereijido, 1978) the major component of the Cl^- fluxes under short-circuit conditions goes *via* a conductive pathway, and the 'trans-effect' observed in these studies was suggested to be due to a $[Cl^-]_o$-dependent decrease in a passive, conductive anion permeability. The small Cl^- efflux in the short-circuited skin of salt-adapted toads is not further reduced after replacement of Cl^- by SO_4^{2-} in the outer solution (Table 3) (see Discussion).

The conductance of skins bathed with K-gluconate Ringer on the outside was reduced from 0·44 ± 0·09 mS cm^{-2} in water-adapted toads to 0·23 ± 0·09 mS cm^{-2} in 250 mM-NaCl-adapted toads (see Table 2), suggesting that the conductance of the leakage pathway is also affected by salt adaptation.

Stimulation of the Cl^- conductance by in vitro *application of a phosphodiesterase inhibitor*

The Cl^- conductance of the skin is increased by serosal application of theophylline in frogs (Cuthbert & Painter, 1968; Mandel, 1975; Kristensen, 1983) and toads (Larsen & Kristensen, 1977). We studied the effect of the xanthine derivative, 3-isobutyl-1-methyl-xanthine (IBMX), which is a potent inhibitor of the phosphodiesterase in rat adrenal cortex (Peytreman *et al.* 1973).

Addition of 1 mM-IBMX to the serosal bath increased the Cl^- conductance in the skin of salt-adapted toads. The time course of stimulation could be studied by recording the response of the clamping current in skins clamped at, say, -100 mV, and bathed with KCl Ringer on the outside. After a delay of 10–15 min the outward clamping current started to increase, achieving a new steady value within 30–45 min after addition of IBMX (not shown). Stimulation occurred with the normal 250 mosmol l^{-1} Ringer at the serosal surface, or the 500 mosmol l^{-1} Ringer.

To study the effect on voltage clamp currents, identical protocols were used during an initial control period (Fig. 7A) and following application of 1 mM-IBMX (Fig. 7B). Prior to IBMX treatment the steady-state outward clamping current at $V = -100$ mV was less than $-10 \mu A$ cm^{-2}. Voltage clamping to -150 mV led to a time-dependent stimulation of the outward current with a delay of more than 30
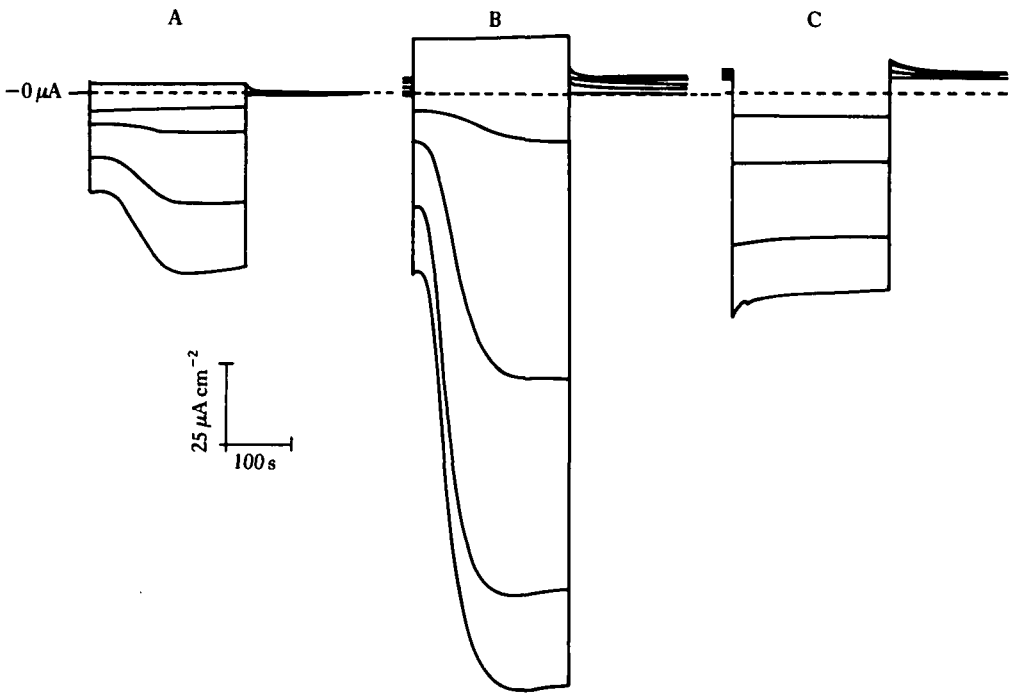
Fig. 7. Voltage clamp currents of a preparation from a fully salt-adapted *Bufo viridis*. Holding potential = 0 mV. The currents were recorded following a shift in V from the holding potential to 50, −50, −100, −150 and −180 mV respectively. Inner solution is toad Ringer of increased NaCl and urea concentration (see Methods). Outside solution is KCl Ringer. (A) Control period. Note the similarity of the current-time curves with those shown in Fig. 6C, despite different composition of serosal solution. (B) Current-time curves of the same preparation as in A, but after addition of 1 mM-IBMX. These records compare with those of Figs 3B and 6A. (C) As in B, but after replacement of the Cl⁻ ions in the outer bath by gluconate.

The steady-state current was small, however, and it corresponded to a trans-epithelial conductance of $0.24 \, \text{mS cm}^{-2}$. Following addition of IBMX, the voltage clamp currents were closer to those obtained in skins of water-adapted toads (compare with Fig. 6A), i.e. the currents were typically time dependent for all $V < 0 \, \text{mV}$, they exhibited a smaller delay of current activation (Fig. 7B), and the time-dependent components disappeared if Cl⁻ ions were omitted from the external bath (Fig. 7C).

Currents could be stimulated by IBMX in the absence of Cl⁻ in the outer bath (Fig. 8), showing that IBMX treatment also affects a leakage pathway of the skin.

Change in number and size of mitochondria-rich cells following salt adaptation of the toad

In water-adapted toads the number of granulosum cells of the replacement layer was about twice that of the m.r. cells (Table 4). Following salt adaptation this ratio was increased to 4, indicating a reduced number of m.r. cells. A certain degree of shrinkage of the m.r. cells was also indicated, as the height of these cells was about ▮0 % reduced, and their width was reduced by about 8 %. This latter finding agrees
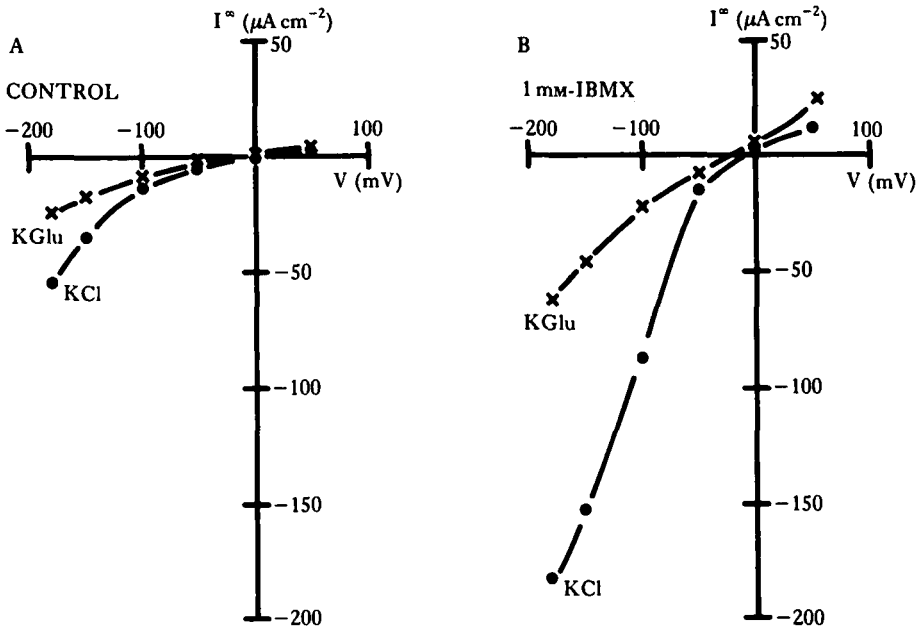
Fig. 8. Steady-state current-voltage curves of the skin of a toad fully adapted to 250 mM-NaCl. Inner solution is toad Ringer of increased NaCl and urea concentration. The major cation of the outer solution is K^+, the major anion being Cl^- or gluconate as indicated on the graphs. (A) Control period prior to IBMX application. (B) Current-voltage curves after addition of 1 mM-IBMX to the inner solution.

Table 4. *Number and size of mitochondria-rich (m.r.) and granulosum (gr.) cells of the replacement layer (the layer of cells beneath stratum corneum) in the belly skin of* Bufo viridis *acclimated in* H_2O *and* 200 mM-NaCl *for 10 days*

	No. of cells per 200 μm			M.r. cells		
Exptl group	m.r. cells (a)	gr. cells (b)	Ratio of a/b	height (h, μm)	width (w, μm)	h × w (μm²)
H_2O	$4·2 \pm 0·7$	$8·4 \pm 0·3$	$0·50 \pm 0·06$	$20·0 \pm 1·1$	$7·5 \pm 0·4$	158 ± 7
200 mM-NaCl	$2·7 \pm 0·3$	$10·6 \pm 0·2$	$0·25 \pm 0·02$	$15·7 \pm 1·5$	$6·9 \pm 0·3$	107 ± 10
Difference (%)	−36	+27	−50	−21·5	−8	−32
P	<0·005	<0·001	<0·001	0·001		<0·001

Mean ± s.e.. Four animals in each group. Four fields of each skin were analysed.

well with the result of an electron microprobe analysis of the intracellular ion and dry mass content of the epithelial cells of *B. viridis* (Rick *et al.* 1980).

DISCUSSION

The experimental protocols of the present study have been directed by the recently developed model of Cl^- transport through amphibian skin, according to which th

pical membrane Cl^- permeability is gated by membrane potential. Thus, characterization of the Cl^- transport includes measurement of Cl^- currents as functions of potential and time in order to obtain steady-state current-voltage curves, conductance-voltage relationships, and time course of permeability activations. It should be noted, however, that the transepithelial voltage clamp method provides limited information on the kinetics of the potential-dependent Cl^- permeability. This is because the slow permeability activation, initiated by a hyperpolarizing potential pulse, is expected to change the outer membrane potential, whereby the rate coefficients of the gating reaction as well as the driving force of the Cl^- current through gated channels change with time. In addition, the ionic currents may change the intracellular ion concentrations, which also disturbs the driving force of ion flow through the apical membrane. The non-steady-state transepithelial clamping currents, associated with the net change of ionic content of the cells, add to the gated current component. The first step in separating the gated current from the ion distribution currents is to eliminate the Na^+ currents by exposure of the external border of the skin to a Na^+-free Ringer's solution. Computer analysis of a mathematical model of the epithelium have indicated that, in this experimental situation, the kinetics of the transepithelial clamping currents are predominantly governed by the Cl^- permeability of the apical membrane (Larsen & Rasmussen, 1982). In the present study the analysis of the time course of clamping currents and the conductance-voltage relationship is carried out with a Na^+-free external solution. With Na^+ ions in the outer solution the Cl^- ion flow was traced by $^{36}Cl^-$ flux measurements.

The skin of water-adapted toads

It has been shown that the Cl^- transport across the skin of water-adapted *B. viridis* exhibits characteristics common to those described in detail for *B. bufo*. The basic features include a small but significant active Cl^- transport in the inward direction, and a passive gated Cl^- conductive path that is activated by hyperpolarization.

The net Cl^- transport at $V = 0\,mV$ in skins exposed to $2\cdot4\,mM$-HCO_3^- Ringer corresponds to $-3\cdot5 \pm 2\cdot7\,\mu A\,cm^{-2}$, not significantly different from zero (Table 1). A value of $I_{Cl} = -20\cdot4 \pm 8\cdot2\,\mu A\,cm^{-2}$ was obtained in skins exposed to $20\,mM$-HCO_3^- Ringer on the serosal side. Also the short-circuit current was significantly (about five times) larger in the $20\,mM$-HCO_3^- skins than in the $2\cdot4\,mM$-HCO_3^- skins. A strong dependence of active Na^+ transport on the serosal HCO_3^--concentration has been reported by Lew (1970), showing that the short-circuit current of the colonic epithelium of *B. arenarium* is reversibly abolished by exposure to a bicarbonate-free Ringer. It was also found that $5\,mM$-HCO_3^- restored at least $50\,\%$ of the short-circuit current which was maximally stimulated by $30\,mM$ serosal HCO_3^-, indicating a significant dependence on small concentrations of this anion. The mechanism of this dependence is not known. It is noteworthy, however, that Lew also showed that the concentration of mucosal bicarbonate did not influence either the transepithelial potential or the short-circuit current of colonic epithelium.

The Cl^- efflux under short-circuit conditions was $16\cdot0 \pm 3\cdot0\,nmol\,cm^{-2}\,min^{-1}$ ($2\cdot4\,mM$-HCO_3^- skins). Provided this flux component is governed by simple passive transport, the associated Cl^- conductance at $V = 0\,mV$ can be calculated from,

$G_{Cl} = F^2 J^{out}_{Cl}/RT$ (Hodgkin, 1951; Ussing & Zerahn, 1951). This gives G_{Cl}
$1\cdot01\ mS\ cm^{-2}$. The skin conductance at $V = 0\ mV$ was $1\cdot6 \pm 0\cdot2\ mS\ cm^{-2}$ (efflux
skins). This is above the estimated Cl^- conductance, and the difference could well be
the conductance of the active Na^+ pathway. With KCl Ringer outside the skin,
conductance at $V = 0\ mV$ (20 mM bicarbonate group) is in the range of $0\cdot5-1\ mS\ cm^{-2}$
(Fig. 5A), and the efflux of Cl^- (Table 3, $V = 0\ mV$) corresponds to $0\cdot57\ mS\ cm^{-2}$.
These calculations show that non-conductive $Cl^-:Cl^-$ exchange diffusion is prob-
ably rather small for both experimental groups. Thus, the 'trans-effect' (Table 3)
might just as well be due to a $[Cl^-]_o$-dependent closure of Cl^- channels (Kristensen,
1978, 1982; Ques-von Petery et al. 1978), as to a depressed Cl^- efflux along an
exchange pathway. The first-mentioned interpretation goes along with the observa-
tion that the conductance becomes stimulated following a shift of V from 50 to 0 mV
(Figs 5A, 6A), indicating the presence of a significant Cl^- conductance at $V =$
0 mV.

The polarity of the gating mechanism has interesting implications for the inter-
dependence of transepithelial Na^+ and Cl^- fluxes (Larsen & Rasmussen, 1983). As
the outer membrane potential depends on the Na^+ current it follows that this quantity
rules the Cl^- permeability. For example, the depolarization of the apical membrane
associated with stimulation of its Na^+ permeability, will also lead to an activation of
the Cl^- permeability. Conversely, if Na^+ permeability is reduced (whereby the apical
membrane is hyperpolarized), the Cl^- permeability becomes deactivated, and passive
loss of Cl^- through the epithelium is prevented. Thus, the gating mechanism operates
in such a way that the Na^+ and Cl^- fluxes appear tightly coupled, although being
carried by separate and specific transport systems.

The skin of salt-adapted toads

Long-term (more than 10 days) acclimation in high salinity results in substantial
changes in Cl^- transport across the isolated skin. The active transport component
disappears, and the fully activated conductance of the gated path is decreased.
Furthermore, the latter needs stronger polarization potentials (below $-100\ mV$ as
compared to $-20\ mV$) to be activated. Taken together with the significantly reduced
Na^+ permeability of the apical membrane (Katz, 1975), these observations suggest
that the skin does not primarily serve NaCl absorption in salt-adapted animals.
Rather, its role in osmoregulation may be related to maintenance of high plasma urea
concentration by a recycling mechanism of the type suggested by Gomme (1981) and
discussed by Katz et al. (1981).

Kristensen (1983) observed that the degree of Cl^- current rectification varies con-
siderably among belly skins of R. esculenta, with some skins exhibiting an almost
linear steady-state I_{Cl}-V relationship. However, addition of theophylline to these skins
evoked the potential-dependent Cl^- current, and it was suggested that theophylline
treatment brings the Cl^- transport system into a cAMP activated state at which it can
be gated by membrane potential. This hypothesis directed us to study the effect of a
phosphodiesterase inhibitor on the Cl^- currents in skins of salt-adapted B. viridis.
Our finding that IBMX treatment restored the potential-dependent Cl^- conductance
indicates that the reduced Cl^- permeability of the skin of salt-adapted toads relies on
a cAMP controlled reaction step. The implication of these findings may be that Cl^-

permeability could be modulated by the action of fast-acting hormones to alter cellular [cAMP]. The identity of such hormones remains to be determined.

Mitochondria-rich cells and chloride transport

The cellular locus of the potential-dependent Cl^- permeability has not been unequivocally established, but data shown in Table 4 and Figs 4–8 indicate that the mitochondria-rich cells are involved. Thus, during adaptation to high salinity, skins show a decrease in V-dependent Cl^- conductance and this is associated with a decrease in number and also size of mitochondria-rich cells. In contrast, the number of granulosum cells increased during salt adaptation. These findings are consistent with those of Voûte & Meier (1978), who found for frog (*R. esculenta*) skin that the passive Cl^- conductance was linearly related to the number of m.r. cells of the replacement layer. Furthermore, it was shown that the mitochondria-rich cells, but not the granulosum cells, swell following exposure of the skin to K-gluconate Ringer on the inside, and KCl Ringer on the outside, and it was concluded that the apical membrane of the m.r. cells, but not that of the granulosum cells, is permeable to Cl^- ions. Ussing (1982) has come to a similar conclusion from studies of the cell volume response to variations of the tonicity and ionic composition of the bathing solutions. Further, studies of Kristensen (1981) have indicated that the active Na^+ transport in frog skin goes along two separated cellular pathways and that only one of these takes part in the transepithelial Cl^- transfer. Finally, in the skin of *B. bufo* the fully activated Cl^- current (measured at $V = -100\,mV$) is positively correlated with the density of m.r. cells (N. Willumsen & E. H. Larsen, unpublished observations). Taken together, the findings of all of these studies provide good evidence that the m.r. cells of amphibian skin are specialized for transepithelial Cl^- uptake.

In the above-mentioned I_{Cl}/m.r. cell-density studies, the statistical analysis relied on the accidental variation of the Cl^- conductance in skins of animals kept under standard laboratory conditions [20 °C, either submerged in (frogs) or having free access to (toads) tap water]. In the present study large variations in Cl^- conductance have been induced by exposure of the animals to solutions of different [NaCl] and osmolarity. The finding that the ratio of m.r. cells and granulosum cells is decreased by a factor of two (Table 4) concomitant with a decrease of the gated Cl^- conductance and disappearance of active Cl^- transport lend support for the hypothesis that, in addition to the above-mentioned metabolic (i.e. by cAMP) regulation, proliferation/ degeneration of m.r. cells occurs as a long-term adjustment of the Cl^- transporting capacity of the toad skin.

A similar role has been established for Cl^- transport by the mitochondria-rich, 'chloride' cells of opercular and skin membranes (Foskett & Scheffey, 1982; Marshall & Nishioka, 1980) and, probably, gill epithelia (e.g. Maetz & Bornancin, 1975) of euryhaline teleosts. Interestingly, for teleosts the m.r. cell serves as a site of *active* Cl^- *secretion*, and the number and size of these cells *increase* during salt adaptation (Foskett *et al.* 1981), while for amphibians the m.r. cell serves as a site of *passive* Cl^- *absorption* (present study), and their number and size *decrease* during salt adaptation. Both types of transport appear to be increased by rapid elevation of cellular levels of cAMP (e.g. see Foskett, Hubbard, Machen & Bern, 1982). In teleosts, cortisol (Foskett *et al.* 1981) and prolactin (Foskett, Machen & Bern, 1982) appear to play

major roles in controlling long-term differentiation of chloride cells. It is likely that hormonal mechanisms also play a role in controlling m.r. cells of amphibians.

REFERENCES

Biber, T. U. L., Walker, T. C. & Mullen, T. L. (1980). Influence of extracellular Cl concentration on Cl transport across isolated skin of *Rana pipiens*. *J. Membr. Biol.* **56**, 81–92.

Bruus, K., Kristensen, P. & Larsen, E. H. (1976). Pathways for chloride and sodium transport across toad skin. *Acta physiol. scand.* **97**, 31–47.

Conway, E. J. (1957). The nature and significance of concentration relations of potassium and sodium in skeletal muscle. *Physiol. Rev.* **37**, 84–132.

Cuthbert, A. W. & Painter, E. (1968). The effect of theophylline on chloride permeability and active chloride transport in various epithelia. *J. Pharm. Pharmac.* **20**, 492–495.

Foskett, J. K., Hubbard, G. M., Machen, T. E. & Bern, H. A. (1982). Effects of epinephrine, glucagon and vasoactive intestinal polypeptide on chloride secretion by teleost opercular membrane. *J. comp. Physiol.* **146**, 27–34.

Foskett, J. K., Logsdon, C. D., Turner, T., Machen, T. E. & Bern, H. A. (1981). Differentiation of the chloride extrusion mechanism during seawater adaptation of a teleost fish, the cichlid *Sarotherodon mossambicus*. *J. exp. Biol.* **93**, 209–224.

Foskett, J. K., Machen, T. E. & Bern, H. A. (1982). Chloride secretion and conductance of teleost opercular membrane. *Am. J. Physiol.* **242**, R380–R389.

Foskett, J. K. & Scheffey, C. (1982). The chloride cell: definitive identification as the salt-secretory cell in teleosts. *Science, N.Y.* **215**, 164–166.

Gomme, J. (1981). Recycling of D-glucose in collagenous cuticle: A means of nutrient conservation? *J. Membr. Biol.* **62**, 47–52.

Hodgkin, A. L. (1951). The ionic basis of electrical activity in nerve and muscle. *Biol. Rev.* **26**, 339–409.

Katz, U. (1973a). Cellular adaptations to hypertonic solution in amphibia adapted to high salinities. Ph.D. thesis, pp. 109. Jerusalem: The Hebrew University.

Katz, U. (1973b). Studies on the adaptation of the toad *Bufo viridis* to high salinities: oxygen consumption, plasma concentration and water content of the tissues. *J. exp. Biol.* **58**, 785–796.

Katz, U. (1975). Salt induced change in sodium transport across the skin of the euryhaline toad *Bufo viridis*. *J. Physiol., Lond.* **247**, 537–550.

Katz, U. (1979). Role of the skin in osmoregulation and in the acid base status of toads (*B. viridis*) under adaptation to high salinity. *INSERM* **85**, 351–358.

Katz, U., Garcia-Romeu, F., Masoni, A. & Isaia, J. (1981). Active transport of urea across the skin of the euryhaline toad, *Bufo viridis*. *Pflügers Arch. ges. Physiol.* **390**, 299–300.

Koefoed-Johnsen, V., Ussing, H. H. & Zerahn, K. (1952). The origin of the short-circuit current in the adrenaline stimulated frog skin. *Acta physiol. scand.* **27**, 38–48.

Kristensen, P. (1978). Effect of amiloride on chloride transport across amphibian epithelia. *J. Membr. Biol.* **40S**, 167–185.

Kristensen, P. (1981). Is chloride transfer in frog skin localized to a special cell type? *Acta physiol. scand.* **113**, 123–124.

Kristensen, P. (1982). Chloride transport in frog skin. In *Chloride Transport in Biological Membranes*, (ed. F. A. Zadunaisky), pp. 319–331. New York: Academic Press.

Kristensen, P. (1983). Exchange diffusion, electrodiffusion and rectification of the chloride transport pathway of frog skin. *J. Membr. Biol.* **72**, 141–151.

KRISTENSEN, P. & LARSEN, E. H. (1978). Relation between chloride exchange diffusion and a conductive chloride pathway across the isolated skin of the toad *Bufo bufo. Acta physiol. scand.* **102**, 22–34.

LARSEN, E. H. (1982). Chloride current rectification in toad skin epithelium. In: *Chloride Transport in Biological Membranes*, (ed. J. A. Zadunaisky), pp. 333–364. New York: Academic Press.

LARSEN, E. H. & KRISTENSEN, P. (1977). Effects of anoxia and of theophylline on transcellular Cl⁻-transport in toad skin. *Proc. int. Union physiol. Sci.* **12**, 1002.

LARSEN, E. H. & KRISTENSEN, P. (1978). Properties of a conductive cellular chloride pathway in the skin of the toad *(Bufo bufo). Acta physiol. scand.* **102**, 1–21.

LARSEN, E. H. & RASMUSSEN, B. E. (1982). Chloride channels in toad skin. *Phil. Trans. R. Soc. Ser. B* **299**, 413–434.

LARSEN, E. H. & RASMUSSEN, B. E. (1983). Membrane potential plays a dual role for chloride transport across toad skin. *Biochim. biophys. Acta.* **728**, 455–459.

LEW, V. L. (1970). Short-circuit current and ionic fluxes in the isolated colonic mucosa of *Bufo arenarium. J. Physiol., Lond.* **206**, 509–528.

MAETZ, J. & BORNANCIN, M. (1975). Biochemical and biophysical aspects of salt secretion by chloride cells in teleosts. *Fortsch. Zool.* **23**, 322–362.

MANDEL, L. O. (1975). Actions of external hypertonic urea, ADH, and theophylline on transcellular and extracellular solute permeabilities in frog skin. *J. gen. Physiol.* **55**, 599–615.

MARSHALL, W. S. & NISHIOKA, R. S. (1980). Relation of mitochondria-rich cells to active chloride transport in the skin of a marine teleost. *J. exp. Zool.* **214**, 147–156.

PEYTREMAN, A., NICHOLSON, W. E., LIDDLE, G. W., HARDMAN, J. G. & SUTHERLAND, E. W. (1973). Effects of methylxanthines on adenosine 2',5'-monophosphate and corticosterone in the rat adrenal. *Endocrinology* **92**, 525–530.

QUES-VON PETERY, M. V., ROTUNNO, C. A. & CEREIJIDO, M. (1978). Studies on chloride permeability of the skin of *Leptodactylus ocellatus*: I. Na⁺ and Cl⁻ effect on passive movement of Cl⁻. *J. Membr. Biol.* **42**, 317–330.

RICK, R., DÖRGE, A., KATZ, U., BAUER, R. & THURAU, K. (1980). The osmotic behaviour of toad skin epithelium *(Bufo viridis)*. An electron microprobe analysis. *Pflügers Arch. ges. Physiol.* **385**, 1–10.

ROTUNNO, C. A., QUES-VON PETERY, M. V. & CEREIJIDO, M. (1978). Studies on chloride permeability of the skin of *Leptodactylus ocellatus*: II. Na⁺ and Cl⁻ effect on inward movements of Cl⁻. *J. Membr. Biol.* **42**, 331–343.

USSING, H. H. (1949). The distinction by means of tracers between active transport and diffusion. *Acta physiol. scand.* **19**, 43–56.

USSING, H. H. (1982). Volume regulation of frog skin epithelium. *Acta physiol. scand.* **114**, 363–369.

USSING, H. H. & ZERAHN, K. (1951). Active transport of sodium as the source of electric current in the short circuited isolated frog skin. *Acta physiol. scand.* **23**, 109–127.

VOÛTE, C. L. & MEIER, W. (1978). The mitochondria-rich cell of frog skin as hormone sensitive 'shunt path'. *J. Membr. Biol.* **40S**, 141–165.

ZADUNAISKY, J. A., CANDIA, O. A. & CHIARANDINI, D. J. (1963). The origin of the short-circuit current in the isolated skin of the South American frog *Leptodactylus ocellatus. J. gen. Physiol.* **47**, 393–402.